

X-ray clusters of galaxies in conformal gravity

Antonaldo Diaferio^{1,2*} and Luisa Ostorero^{1,2,*}

¹*Dipartimento di Fisica Generale “Amedeo Avogadro”, Università degli Studi di Torino, Via P. Giuria 1, I-10125, Torino, Italy*

²*Istituto Nazionale di Fisica Nucleare (INFN), Sezione di Torino, Via P. Giuria 1, I-10125, Torino, Italy*

7 September 2021

ABSTRACT

We run adiabatic N -body/hydrodynamical simulations of isolated self-gravitating gas clouds to test whether conformal gravity, an alternative theory to General Relativity, is able to explain the properties of X-ray galaxy clusters without resorting to dark matter. We show that the gas clouds rapidly reach equilibrium with a density profile which is well fit by a β -model whose normalization and slope are in approximate agreement with observations. However, conformal gravity fails to yield the observed thermal properties of the gas cloud: (i) the mean temperature is at least an order of magnitude larger than observed; (ii) the temperature profiles increase with the square of the distance from the cluster center, in clear disagreement with real X-ray clusters. These results depend on a gravitational potential whose parameters reproduce the velocity rotation curves of spiral galaxies. However, this parametrization stands on an arbitrarily chosen conformal factor. It remains to be seen whether a different conformal factor, specified by a spontaneous breaking of the conformal symmetry, can reconcile this theory with observations.

Key words: gravitation – methods: N -body simulations – galaxies: clusters: general – dark matter – X-ray: galaxies: clusters.

1 INTRODUCTION

On the scale of individual galaxies and larger scales, General Relativity requires large amounts of dark matter to describe the dynamics of cosmic structure. Moreover, the late-time acceleration of the Hubble expansion implies the existence of a cosmological constant, a special case of a dark energy fluid which is suggested by more sophisticated models (see Copeland et al. 2006, for a review). In principle, we can avoid the dark matter and dark energy solutions to the puzzles posed by the astrophysical data by adopting an alternative theory of gravity, which reduces to General Relativity in the appropriate limit. Independently of the dark matter and dark energy problems, a modification of General Relativity is also highly desirable if we ultimately wish to unify gravity with the other fundamental interactions.

Possible modifications of the Einstein-Hilbert action proposed in the literature are, among others, (i) the introduction of additional scalar and/or vector fields (e.g., Fujii & Maeda 2003; Bekenstein 2006); (ii) the assumption of arbitrary functions $f(R)$ of the Ricci scalar R (e.g., Capozziello & Francaviglia 2008; Nojiri & Odintsov 2008); (iii) the introduction of additional dimensions to the four di-

mensions of the General Relativity spacetime manifold (e.g., Maartens 2004).

A different approach was suggested by Mannheim (1990) who revived Weyl’s theory (Weyl 1918, 1919, 1920) as a possible candidate to solve the dark matter and dark energy problems. When the geometry is kept Riemannian, with a null covariant derivative of the metric tensor, we can obtain a milder version of Weyl’s gravity, known as conformal gravity. In this theory, we impose a local conformal invariance on the gravitational field action in the curved four-dimensional spacetime. The Einstein-Hilbert Lagrangian density for the gravitational field is chosen on the requirement that the theory of gravity is a second-order derivative theory. In conformal gravity, the Lagrangian density is chosen on the principle of local conformal symmetry which is uniquely satisfied by the action $I_W = -\alpha \int d^4x \sqrt{-g} C_{\mu\nu\kappa\lambda} C^{\mu\nu\kappa\lambda}$, where $C_{\mu\nu\kappa\lambda}$ is the Weyl tensor, α is a coupling constant, and g is the determinant of the metric tensor $g_{\mu\nu}$. Conformal symmetry is guaranteed by the invariance of the Weyl tensor to local conformal transformations $g_{\mu\nu}(x) \rightarrow \Omega^2(x)g_{\mu\nu}(x)$, where $\Omega^2(x)$ is an arbitrary conformal factor that can be specified by a spontaneous breaking of the conformal invariance (Edery et al. 2006; Mannheim 2008b). The theory of gravity implied by the action I_W is a fourth-order derivative theory. The vacuum exterior solution for a static and spherically symmetric spacetime contains the

* E-mail: diaferio@ph.unito.it (AD); ostorero@ph.unito.it (LO)

Schwarzschild solution (Mannheim & Kazanas 1989). The weak-field limit is consistent with the Solar System observational data (Mannheim 2007), unlike claimed in previous investigations (Barabash & Shtanov 1999; Flanagan 2006; Barabash & Pyatkovska 2007).

Mannheim (1993, 1997) shows that conformal gravity can reproduce the rotation curves of disc galaxies without dark matter. Moreover, conformal gravity can explain the current accelerated expansion of the universe without resorting to a fine-tuned cosmological constant or to the existence of dark energy (Mannheim 2001, 2003; Varieschi 2008). Unlike the standard theory, where the universe starts accelerating at redshift $z \lesssim 1$, conformal gravity predicts that the universe is accelerating at all times. Therefore, observational data probing the Hubble plot at very high redshift (e.g., Navia et al. 2008; Wei & Zhang 2008) can be a decisive test.

More recently, conformal theory has been proposed as a valid candidate for building a theory of quantum gravity (Mannheim 2008a); in fact, theories based on fourth-order derivative equations of motion have had the long-lasting problem of suffering from the presence of ghosts. Bender & Mannheim (2008) have recently shown that this erroneous belief is the result of considering the canonical conjugates \mathbf{p} of the generic dynamical variables \mathbf{q} , when the \mathbf{q} 's are real, to be Hermitian operators; however, this assumption is incorrect, and when the non-Hermiticity property of the Hamiltonian of these higher-order quantum field theories is correctly taken into account, the states with negative norm disappear.

From an astrophysical perspective, however, the form of conformal gravity that has been proposed in the literature currently has two main shortcomings: the abundance of light elements, and the gravitational lensing phenomenology.

Conformal gravity nicely avoids the requirement of an initial Big Bang singularity, but it still predicts an early universe sufficiently dense and hot to ignite the light element nucleosynthesis. However, conformal gravity predicts a too slow initial expansion rate. This rate favours the destruction of most of the deuterium produced in the early universe (Knox & Kosowsky 1993; Elizondo & Yepes 1994) and poses conformal gravity in serious difficulties compared to the standard Big Bang nucleosynthesis. Conformal gravity necessarily requires astrophysical processes for the production of the deuterium currently observed, for example neutron radiative capture on protons in the atmospheres of active stars (Mullan & Linsky 1999) or gamma-ray bursts (Inoue et al. 2003). However, the processes investigated to date do not seem to be efficient enough. For example, significant production of deuterium in the Galaxy seems to be ruled out (Prodanovic & Fields 2003).

The second open issue is the conformal gravity prediction of gravitational lensing. Early investigations of gravitational lensing in conformal gravity (Walker 1994; Ederly & Paranjape 1998, 1999; Ederly 1999) show that, in the weak-field limit, the deflection angle due to a point mass M is $\Delta\alpha = 4GM/c^2r - \gamma r$, where r is the radius of the photon closest approach; $\Delta\alpha$ contains the additional term γr when compared to the General Relativity result. The constant γ has to be positive to fit the galaxy rotation curves, thus implying a repulsive effect in gravitational lensing. It was later realized (Ederly et al. 2001) that the geodesics of

photons are independent of the conformal factor $\Omega^2(x)$ and one can choose an appropriate conformal factor and a radial coordinate transformation to yield attractive geodesics for both massive and massless particles. However, in the strong-field limit, the light deflection might still be divergent or even impossible (Pireaux 2004a,b).

Until these open questions are completely settled, conformal gravity cannot yet be considered ruled out by observations. Moreover, conformal invariance plays a crucial role in elementary particle physics and a viable theory of gravity that includes this property can at least be suggestive of a relevant route towards the unification of the fundamental interactions.

From the astrophysical point of view, conformal gravity can be further tested by investigating the formation of cosmic structure. To date, nobody has yet explored how the large-scale structure forms in conformal gravity. If structures form by gravitational instability, as in the standard theory, the development of a cosmological perturbation theory, which is still lacking, becomes inevitable. This theory would enable the comparison of conformal gravity with the spectrum of the Cosmic Microwave Background anisotropies and would provide initial conditions for the simulation of the structure evolution into the non-linear regime.

Before building up such a theory, however, it is useful to check whether conformal gravity is able to reproduce the equilibrium configuration of cosmic structures, other than galaxies, without dark matter. Horne (2006) has already shown that, if we interpret the observational data of the intracluster medium of X-ray clusters by assuming hydrostatic equilibrium, conformal gravity requires a factor of ten less baryonic mass than inferred from the X-ray surface brightness measures. Here, we extend this analysis by performing hydrodynamical simulations of self-gravitating gas clouds. We modify a standard Tree+SPH code to perform numerical simulations of self-gravitating systems in conformal gravity. The numerical tool we create is extremely relevant if we eventually wish to investigate the formation of the large-scale structure, because we will massively need to resort to numerical integrations when the evolution of the density perturbations reaches the non-linear regime.

In Section 2, we review the basic steps leading to the gravitational potential of a static point source in conformal gravity. In Section 3, inspired by the analysis of Horne (2006), we compute the gravitational potential energy of a spherical system, and in Section 4 we use this result to compute the expected mean temperature and the temperature profile of the intracluster medium. In Section 5, we derive the same results with hydrodynamical simulations of self-gravitating gas clouds.

2 CONFORMAL GRAVITY

Conformal gravity is a theory of gravity based on the action $I_W = -\alpha \int d^4x \sqrt{-g} C_{\mu\nu\kappa\lambda} C^{\mu\nu\kappa\lambda}$. For any finite, positive, non-vanishing, continuous, real function $\Omega^2(x)$ of the four spacetime coordinates x , this theory is invariant for any conformal transformation $g_{\mu\nu}(x) \rightarrow \Omega^2(x)g_{\mu\nu}(x)$, because the Weyl tensor is invariant for these transformations. The variational principle applied to the action leads to fourth-order field equations, whose solution for the vacuum exterior to a

static point source leads to the line element

$$ds^2 = \Omega^2(x) \left\{ \left[1 + \frac{2\phi(r)}{c^2} \right] c^2 dt^2 - \left[1 + \frac{2\phi(r)}{c^2} \right]^{-1} dr^2 - r^2 (d\theta^2 + \sin^2 \theta d\phi^2) \right\} \quad (1)$$

where c is the speed of light,

$$\frac{\phi(r)}{c^2} = -\frac{\beta(2-3\beta\gamma)}{2r} - \frac{3}{2}\beta\gamma + \frac{\gamma}{2}r - \frac{k}{2}r^2, \quad (2)$$

and β , γ and k are three integration constants. The arbitrary function $\Omega^2(x)$ can be specified by a mechanism which breaks the conformal symmetry. Mannheim & Kazanas (1989) implicitly assume $\Omega^2(x) = 1$.

According to this assumption, when $\gamma = k = 0$, the metric (2) reduces to the usual Schwarzschild metric with $\beta = GM/c^2$, M the gravitational mass of the point source and G the gravitational constant. The term $kr^2/2$ corresponds to a cosmological solution which is conformal to a Robertson-Walker background; therefore, k can be chosen small enough that it can be neglected on the scales of galaxies and galaxy clusters, and we will not consider this term hereafter. Moreover, the rotation velocities of spiral galaxies suggest a value of γ sufficiently small that the terms proportional to $\beta\gamma \propto \gamma/c^2$ can be safely ignored (Mannheim 1993). Equation (2) thus reduces to

$$\frac{\phi(r)}{c^2} = -\frac{\beta}{r} + \frac{\gamma}{2}r. \quad (3)$$

Mannheim (1997) uses the observed rotation curves of eleven spiral galaxies of widely different luminosities to constrain γ . It turns out that γ also depends on the point source mass M . Mannheim (1997) suggests the parametrization $\gamma = \gamma_0 + M\gamma_*$, where $\gamma_0 = 3.06 \times 10^{-28} \text{ m}^{-1}$ and $\gamma_* = 5.42 \times 10^{-39} \text{ m}^{-1} M_\odot^{-1}$; γ_0 and γ_* should be two universal physical constants. In the following, we adopt a more convenient form of the potential (3) suggested by Horne (2006):

$$\phi(r) = -\frac{GM}{r} + \frac{GM}{R_0^2}r + \frac{GM_0}{R_0^2}r \quad (4)$$

where $M_0 = (\gamma_0/\gamma_*)M_\odot = 5.6 \times 10^{10}M_\odot$ and $R_0 = (2GM_\odot/\gamma_*c^2)^{1/2} = 24 \text{ kpc}$.

3 GRAVITATIONAL POTENTIAL ENERGY OF A SPHERICAL SYSTEM

The gravitational potential of a point source (equation 4)

$$\phi_{ps}(r) = \phi_N(r) + \phi_{CM}(r) + \phi_{CC}(r), \quad (5)$$

with $\phi_N(r) = -GM/r$ the usual Newtonian potential, $\phi_{CM}(r) = GMr/R_0^2$, and $\phi_{CC}(r) = GM_0r/R_0^2$, generates the acceleration

$$g_{ps}(r) = -\nabla\phi_{ps} = -\frac{GM}{r^2} - \frac{GM}{R_0^2} - \frac{GM_0}{R_0^2}. \quad (6)$$

The last term is a constant acceleration independent of the mass of the source of the gravitational field. The physical origin of this term is very subtle. Unlike in Newtonian gravity, the presence of the linear term $\phi_{CM}(r)$ clearly prevents us from neglecting the contribution of distant objects to the acceleration of any body in the universe. According to

Mannheim (1997, 2006), in conformal gravity the net effect of all the mass in the universe is to contribute a constant acceleration in addition to the acceleration due to a local source. Mannheim (1997) shows that, with an appropriate coordinate transformation allowed by the conformal invariance, the mass in the universe exactly generates the additional linear potential $\phi_{CC}(r)$, that we name the *curvature potential*.

This argument implies that, to compute the gravitational potential energy of an extended source, we need to treat the *curvature potential* $\phi_{CC}(r)$ and the potential $\phi_N(r) + \phi_{CM}(r)$, originated by the local field source, separately. For the time being, let us consider this latter gravitational potential alone.

Consider an extended source. The gravitational potential energy of two of its mass elements with separation \mathbf{r} is $dW_{AB} = dm_A dm_B f(\mathbf{r})$, where $f(\mathbf{r})$ is the part of the potential $\phi(\mathbf{r})$ that depends on \mathbf{r} only. When we sum over all the mass elements, we get the total gravitational potential energy $W = (1/2) \int dm_A \int dm_B f(\mathbf{r})$, namely

$$W = \frac{1}{2} \int \phi(\mathbf{r}) \rho(\mathbf{r}) d^3\mathbf{r}, \quad (7)$$

where $\rho(\mathbf{r})$ is the mass density distribution of the source and $\phi(\mathbf{r}) = \phi_N(\mathbf{r}) + \phi_{CM}(\mathbf{r})$ is the gravitational potential generated by its self-gravity alone.

The total potential energy W can also be derived with a different argument which provides an alternative expression to equation (7). For a system of N particles with position \mathbf{r}_i and mass m_i , each feeling a force $\mathbf{F}(\mathbf{r}_i)$, we can define the virial $\sum_i \mathbf{r}_i \cdot \mathbf{F}(\mathbf{r}_i)$; the force is $\mathbf{F}(\mathbf{r}_i) = -m_i \sum_j \nabla_{\mathbf{r}_{ij}} \phi(\mathbf{r}_{ij})$ where $\mathbf{r}_{ij} = \mathbf{r}_i - \mathbf{r}_j$. Now, $m_i \nabla_{\mathbf{r}_{ij}} \phi(\mathbf{r}_{ij}) = -m_j \nabla_{\mathbf{r}_{ji}} \phi(\mathbf{r}_{ji})$ for Newton's third law, and we can write

$$\begin{aligned} \sum_i \mathbf{r}_i \cdot \mathbf{F}(\mathbf{r}_i) &= -\sum_i m_i \sum_{j < i} \mathbf{r}_i \cdot \nabla_{\mathbf{r}_{ij}} \phi(\mathbf{r}_{ij}) + \\ &\quad + \sum_i m_i \sum_{j > i} \mathbf{r}_j \cdot \nabla_{\mathbf{r}_{ij}} \phi(\mathbf{r}_{ij}) \\ &= -\sum_i m_i \sum_{j < i} \mathbf{r}_{ij} \cdot \nabla_{\mathbf{r}_{ij}} \phi(\mathbf{r}_{ij}), \end{aligned} \quad (8)$$

since $\nabla_{\mathbf{r}_{ij}} \phi(\mathbf{r}_{ij}) = 0$ when $j = i$.

Homogeneous functions of order λ of M variables $(\mathbf{x}_1, \dots, \mathbf{x}_M)$ are defined by the relation

$$f(\alpha\mathbf{x}_1, \dots, \alpha\mathbf{x}_M) = \alpha^\lambda f(\mathbf{x}_1, \dots, \mathbf{x}_M) \quad (9)$$

for any non-null α ; they satisfy Euler's theorem

$$\sum_i \mathbf{x}_i \cdot \nabla_{\mathbf{x}_i} f(\mathbf{x}_1, \dots, \mathbf{x}_M) = \lambda f(\mathbf{x}_1, \dots, \mathbf{x}_M). \quad (10)$$

In the potential $\phi = \phi_N + \phi_{CM}$, ϕ_N and ϕ_{CM} are homogeneous functions of order $\lambda_N = -1$ and $\lambda_{CM} = 1$ respectively. By applying Euler's theorem for $M = 1$, we can thus write

$$\begin{aligned} \sum_i \mathbf{r}_i \cdot \mathbf{F}(\mathbf{r}_i) &= -\sum_i \sum_{j < i} m_i [-\phi_N(\mathbf{r}_{ij}) + \phi_{CM}(\mathbf{r}_{ij})] \\ &= W_N - W_{CM}. \end{aligned} \quad (11)$$

Now, $W = W_N + W_{CM}$ and we obtain $W = 2W_N - \sum_i \mathbf{r}_i \cdot \mathbf{F}(\mathbf{r}_i)$. In the continuous limit

$$W = 2W_N + \int \rho(\mathbf{r}) \mathbf{r} \cdot \nabla \phi(\mathbf{r}) d^3\mathbf{r}. \quad (12)$$

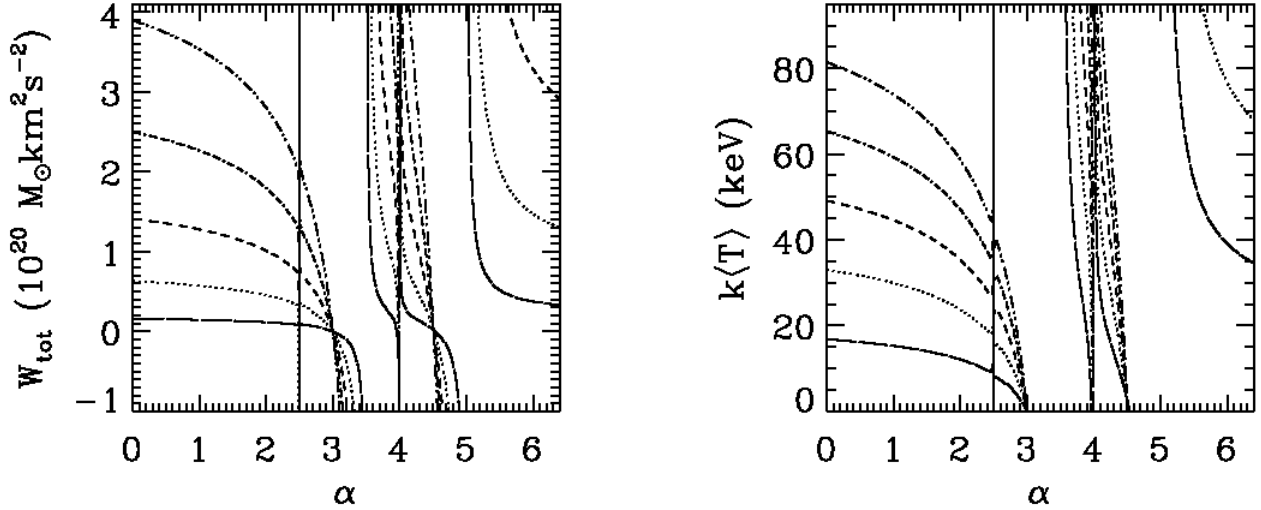


Figure 1. Left panel: Total gravitational potential energy of a spherical system with a power-law density profile $\rho \propto r^{-\alpha}$, radius $a = 1$ Mpc, and mass $M = 2 \times 10^{12} M_{\odot}$ (solid line), $4 \times 10^{12} M_{\odot}$ (dotted line), $6 \times 10^{12} M_{\odot}$ (dashed line), $8 \times 10^{12} M_{\odot}$ (dot-dashed line), $10^{13} M_{\odot}$ (dot-dot-dot-dashed line); see Section 3 for details. Right panel: The mean gas temperature of the systems shown in the left panel according to the virial theorem; see Section 4 for details.

To compute the gravitational potential $\phi(r)$ of a self-gravitating spherical system, we follow Horne (2006) and we first consider a homogeneous spherical shell of density ρ , radius R and mass $m = 4\pi\rho R^2 dR$. At a generic point in space of coordinate \mathbf{r} , each mass element $\delta m = \rho R^2 \sin\theta dR d\theta d\varphi$ of the shell generates the potential $\delta\phi(r)$ given by equation (5). By setting the coordinate system such that $\mathbf{r} = (0, 0, r)$ without loss of generality, the element δm has coordinates $R(\cos\varphi \sin\theta, \sin\varphi \sin\theta, \cos\theta)$ and generates the potential at \mathbf{r}

$$\delta\phi(\mathbf{r}) = G\rho R^2 \sin\theta dR d\theta d\varphi \left(-\frac{1}{x} + \frac{x}{R_0^2} \right), \quad (13)$$

where $x^2 = R^2 + r^2 - 2rR\cos\theta$. By integrating over $d\theta d\varphi$, we find the potential of the shell

$$\phi_{sh}(r) = Gm \begin{cases} -\frac{1}{R} + \frac{1}{R_0^2} \left(\frac{r^2}{3R} + R \right) & r < R \\ -\frac{1}{r} + \frac{1}{R_0^2} \left(\frac{R^2}{3r} + r \right) & r > R. \end{cases} \quad (14)$$

The gravitational potential of a self-gravitating sphere is thus

$$\frac{\phi(r)}{G} = -\frac{I_0(r)}{r} - E_{-1}(r) + \frac{1}{R_0^2} \left[\frac{I_2(r)}{3r} + rI_0(r) + \frac{r^2}{3} E_{-1}(r) + E_1(r) \right] \quad (15)$$

where $I_n(r) = 4\pi \int_0^r \rho(x)x^{n+2} dx$ and $E_n(r) = 4\pi \int_r^{+\infty} \rho(x)x^{n+2} dx$, and the acceleration is

$$-\frac{\nabla\phi(r)}{G} = -\frac{I_0(r)}{r^2} + \frac{1}{R_0^2} \left[\frac{I_2(r)}{3r^2} - \frac{2}{3} r E_{-1}(r) - I_0(r) \right]. \quad (16)$$

The total gravitational potential W of a sphere can now be computed with either equation (7) or equation (12). For a power-law density profile $\rho(r) = \rho_0(r/a)^{-\alpha}$ of a system truncated at radius a with total mass $M = 4\pi\rho_0 a^3/(3-\alpha)$, with

$\alpha \neq 3$, we find $I_0(r) = M(r/a)^{3-\alpha}$, $I_2(r) = [(3-\alpha)/(5-\alpha)]Ma^2(r/a)^{5-\alpha}$, $E_{-1}(r) = [(3-\alpha)/(2-\alpha)](M/a)[1 - (r/a)^{2-\alpha}]$, and $E_1(r) = Ma(3-\alpha)/(4-\alpha)[1 - (r/a)^{4-\alpha}]$, and the gravitational potential energy is

$$W = W_N \left[1 - \left(\frac{a}{R_0} \right)^2 \frac{2(5-2\alpha)(9-2\alpha)}{3(7-2\alpha)(5-\alpha)} \right] \equiv W_N [1 - h(\alpha)]; \quad (17)$$

here

$$W_N = -\frac{GM^2}{a} \frac{3-\alpha}{5-2\alpha} \quad (18)$$

is the potential energy in Newtonian gravity, that is recovered in the limit $R_0 \rightarrow \infty$.

To compute the contribution W_{curv} of the curvature acceleration $-GM_0/R_0^2$ to be added to W , we can use either equation (12) or equation (7) without the factor (1/2), because the *curvature* mass M_0 is *not* accelerated by the mass $\rho(\mathbf{r})d^3\mathbf{r}$. We find

$$W_{\text{curv}} = GM M_0 \frac{a}{R_0^2} \frac{3-\alpha}{4-\alpha} = -W_N \left(\frac{a}{R_0} \right)^2 \frac{M_0}{M} \frac{5-2\alpha}{4-\alpha}. \quad (19)$$

The left panel of Figure 1 shows the total gravitational potential energy

$$W_{\text{tot}} = W_N(\alpha)[1 - h(\alpha)] + W_{\text{curv}}(\alpha) \quad (20)$$

of a spherical system as a function of α and its total mass M . When $\alpha \rightarrow 2.5, 3.5, 4$ and 5 , $W_{\text{tot}} \rightarrow \pm\infty$. In Figure 1, the pole of W_N at $\alpha = 2.5$ seems to have different properties than the other poles, but it is only a graphic artifact. In fact, the contribution of conformal gravity to W_{tot} is proportional to $(a/R_0)^2 \sim 10^3$, and it always dominates the newtonian W_N : we must have $|\alpha - 2.5| \ll 10^{-3}$ to see $W_{\text{tot}} \rightarrow \pm\infty$.

Finally, the ratio between the curvature potential and the conformal gravity potential due to the sphere self-gravity is $\sim M_0/M$; therefore, W_{curv} is negligible when $M \gg M_0$, as in our case, where $M_0/M \sim 10^{-2}$, unless, of course, $\alpha \rightarrow 4$.

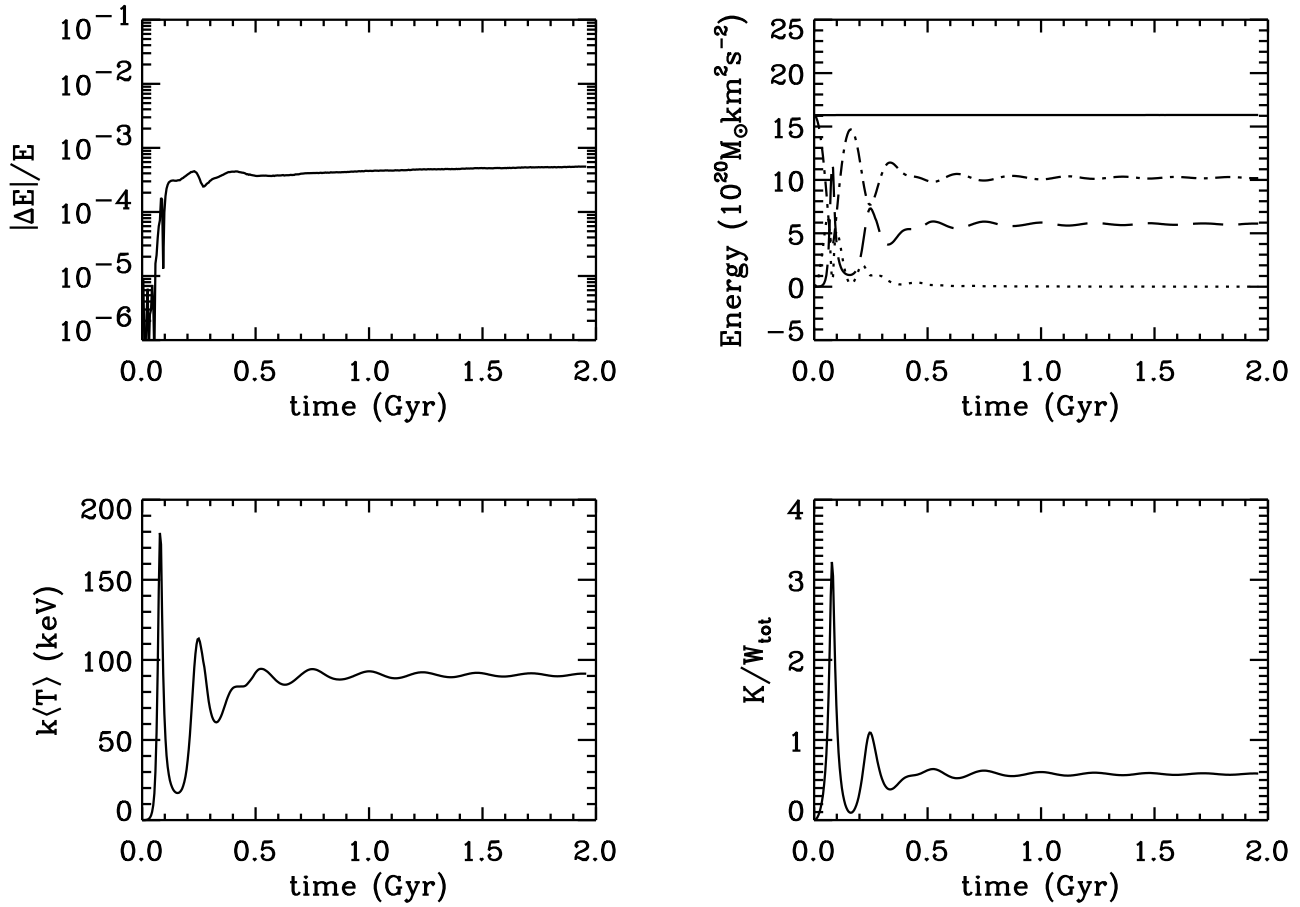


Figure 2. Upper left panel: Fluctuations of the total energy. Upper right panel: Evolution of the kinetic (dotted line), thermal (dashed line), gravitational potential (dot-dashed line), and total (solid line) energy. Lower left panel: Evolution of the mass-weighted mean X-ray temperature. Lower right panel: Evolution of the virial ratio.

4 X-RAY CLUSTERS

A system of N particles of position \mathbf{r}_i experiencing the force \mathbf{F}_i is in virial equilibrium when it satisfies the virial theorem relation $2K + \sum \mathbf{r}_i \cdot \mathbf{F}_i = 0$, where K is the total kinetic energy of the system. We saw above (equation 11) that $\sum \mathbf{r}_i \cdot \mathbf{F}_i = 2W_N - W_{\text{tot}}$ in conformal gravity. Note that we replaced W_{CM} with W_{tot} to include the curvature potential.

Observations indicate that in X-ray clusters the total mass of galaxies is roughly ten times smaller than the total mass of the intracluster medium (e.g., White et al. 1993). We can therefore model X-ray clusters as individual clouds of hot gas with no galaxies and, of course, with no dark matter. This approximation is partly inappropriate for cD clusters, where the contribution of the cD galaxy to the gravitational potential in the cluster center is relevant; however, cD clusters are $\sim 20\%$ of the population of nearby clusters (Rood & Sastry 1971) and our analysis should be valid for most clusters.

If the gas bulk flows and turbulent motions are negligible, the total kinetic energy is $K = (3/2)(\gamma - 1)U = (3/2)Mk\langle T\rangle/\mu m_p$, where $U = [M/(\gamma - 1)]k\langle T\rangle/\mu m_p$ is the internal energy of the gas of density $\rho(\mathbf{r})$, M is the gas total

mass, $\langle T\rangle = \int \rho(\mathbf{r})T(\mathbf{r})d^3\mathbf{r}/\int \rho(\mathbf{r})d^3\mathbf{r}$ is its mass-weighted mean temperature, k the Boltzmann constant, m_p the proton mass, μ the mean molecular weight, and γ the adiabatic index. The virial theorem¹ thus yields

$$k\langle T\rangle = -\frac{\mu m_p}{3M}(2W_N - W_{\text{tot}}) \quad (21)$$

Figure 1 shows the mean temperatures $k\langle T\rangle$ of spherical systems with a power-law density profile as a function of α and its total mass M .

Consider an isothermal sphere with $\alpha = 2$, radius $a = 1$ Mpc, and mass $M = 10^{13}M_\odot$. Newtonian gravity predicts $k\langle T\rangle = 0.09$ keV. Conformal gravity predicts $k\langle T\rangle = 58.21$ keV, namely a temperature $(a/R_0)^2 \sim 10^3$ larger. To explain a more typical temperature of, say, $k\langle T\rangle \sim 6$ keV without resorting to dark matter, the gas mass should be $M \sim 10^{12}M_\odot$, a factor of ten lower than the mass of the intracluster medium measured from the X-ray surface brightness.

This result agrees with the claim of Horne (2006) that the acceleration provided by the conformal gravity potential

¹ The virial theorem can also be generalized in $f(R)$ gravities (Böhmer et al. 2008).

is too intense. We now show that the disagreement with observations extends to the temperature profile, besides its normalization.

To compute the temperature profile of a self-gravitating spherical system in equilibrium, we need to solve the Boltzmann equation coupled to the Poisson equation. In conformal gravity, the Poisson equation $\nabla^2\phi = 4\pi G\rho$ is replaced by a fourth order equation $\nabla^4\phi \propto \rho$ (Mannheim & Kazanas 1994). Following this approach is not a trivial task, either analytically or numerically. In the next section, we resort to a smoothed-particle-hydrodynamical simulation to obtain a self-consistent solution to this problem.

In this section, to illustrate qualitatively the expected result, we can consider the first moment of the Boltzmann equation, namely the Euler equation, which, in hydrostatic equilibrium, reduces to the relation $\nabla p = -\rho\nabla\phi$, where p is the gas pressure. Provided that the density profile $\rho(r)$ is known, for an ideal gas with equation of state $p = \rho kT/\mu m_p$, this equation immediately integrates to

$$\frac{kT(r)}{\mu m_p} = -\frac{1}{\rho(r)} \left[\int \rho(r)\nabla\phi(r)dr + A_0 \right] \quad (22)$$

where A_0 is an integration constant. At large radii, real clusters usually have the intracluster medium density profile which decreases more rapidly than the temperature profile. This constraint requires that the term $A_0/\rho(r)$ should disappear at large radii and implies $A_0 = 0$. For a power-law density profile, we find

$$T(r) = T_N(r) \left\{ 1 + \frac{\alpha-1}{(2-\alpha)^2} \left(\frac{a}{R_0} \right)^2 \left[\frac{2}{(5-\alpha)} \left(\frac{r}{a} \right)^2 - \frac{4(3-\alpha)}{3} \left(\frac{r}{a} \right)^\alpha \right] \right\} + \frac{GM_0}{R_0} \frac{1}{1-\alpha} \left(\frac{r}{R_0} \right) \quad (23)$$

where

$$\frac{kT_N(r)}{\mu m_p} = \frac{GM}{2a} \frac{1}{\alpha-1} \left(\frac{r}{a} \right)^{2-\alpha}. \quad (24)$$

Note that for an isothermal sphere ($\alpha = 2$) in Newtonian gravity, this equation yields $kT_N/\mu m_p = GM/2a$. This temperature disagrees with the correct virial theorem result $kT_N/\mu m_p = GM/3a$ (equation 21). This discrepancy is a simple consequence of the inconsistent approach we used to obtain equation (23). However, we can use equation (23) to predict that, at large radii, the temperature profile increases at least as r^2 .

We thus conclude that the values of the conformal physical constants $R_0 = 24$ kpc and $M_0 = 5.6 \times 10^{10} M_\odot$ implied by the galaxy rotation curves provide X-ray clusters with average temperatures a factor of ten too large, and rising temperature profiles, clearly at odds with real clusters.

5 NUMERICAL SOLUTION

To solve properly the coupled Boltzmann and Poisson equations and predict the correct X-ray properties of a galaxy cluster in conformal gravity, we run hydrodynamical simulations of isolated spheres of gas with a Smoothed-Particle-Hydrodynamic (SPH) code. We use a modified version of the publicly available GADGET-1.1 code (Springel et al. 2001; Springel 2005). The original version of GADGET-1.1 is a Tree+SPH code which integrates the equations of motion

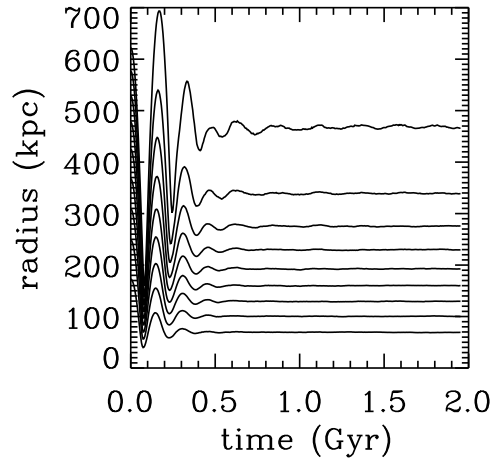


Figure 3. Evolution of the size of the gas cloud: From bottom to top, lines are for radii containing 10% to 90% of the total cloud mass.

of N particles which interact gravitationally. The N particles are a discrete representation of either a collisionless or a collisional fluid; traditional simulations contain both collisionless and collisional particles which represent the dark matter and the baryonic fluids, respectively.

In our simulations, we only require the presence of the baryonic fluid and we only have collisional particles. Moreover, in Newtonian gravity, the potential between two particles decreases with the interparticle distance, and GADGET-1.1 arranges the particles in a tree structure in order to average the contribution of distant particles to the local acceleration. This technique substantially decreases the time required to compute the acceleration of individual particles. Unfortunately, in conformal gravity this technique can not be applied, because the gravitational potential contains a term that increases linearly with the interparticle distance, and the contribution of distant particles to the gravitational potential must be computed individually. We will therefore use GADGET-1.1 as a direct N -body integrator. The computational cost thus increases with N^2 rather than $N \ln N$. In appendix A, we describe in detail the modification we introduced in GADGET-1.1 to compute the interparticle forces in conformal gravity.

We simulate the evolution of isolated spherical clouds of gas with vacuum boundary conditions. We neglect radiative cooling. At the end of this section we discuss how simulating the gas physics more realistically can actually be relevant to find a way to alleviate the discrepancy between conformal gravity and the observed thermal properties of X-ray clusters.

A gas cloud is represented by $N = 4096$ gas particles. The chosen N is substantially smaller than state-of-the-art simulations of galaxy clusters and is due to the N^2 scaling of the computational cost. We do not actually need a larger N , because the aim of our simulations is to test the general viability of conformal gravity rather than the detailed physics of the intracluster medium, which would require higher spatial and mass resolutions. In fact, the current form of the conformal gravitational potential yields clusters so different

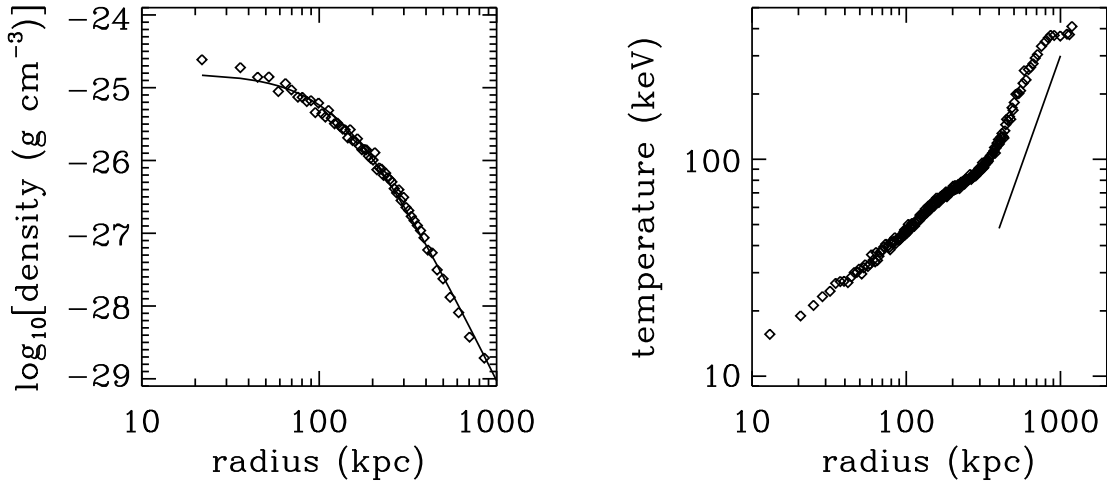


Figure 4. Mass density (left panel) and temperature (right panel) profiles of the final configuration of the gas cloud. The solid line in the left panel is the best-fit β -model profile. The straight line in the right panel shows the $T \propto r^2$ slope.

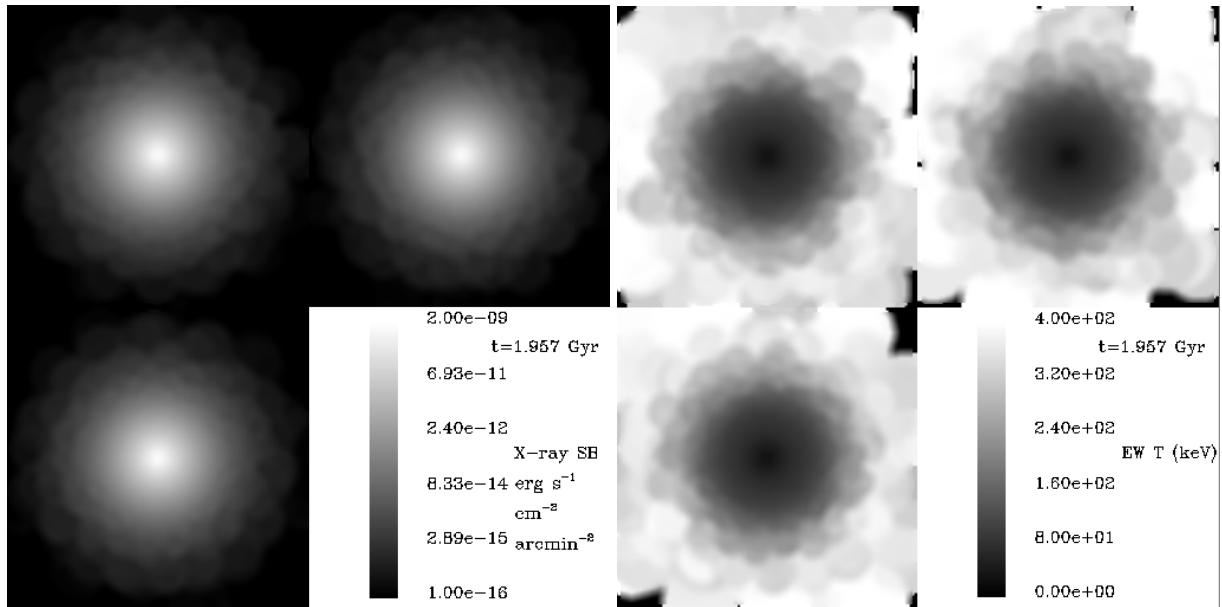


Figure 5. X-ray surface brightness (SB) (left panel) and emission weighted (EW) temperature (right panel) maps of the final configuration of the gas cloud. Each panel shows three orthogonal projections. Each map is 2 Mpc on a side.

from real clusters that running costly simulations is unwarranted.

The gas cloud initially has a β -model density profile

$$\rho(r) = \rho_0 \left[1 + \left(\frac{r}{r_0} \right)^2 \right]^{-3\beta/2} \quad (25)$$

and null thermal and kinetic energies. Each gas particle has gravitational softening length $\epsilon = 0.1$ kpc. Each gas particle also has an individual SPH softening parameter h used to estimate the thermodynamical quantities, as mentioned below; the sphere with radius h centered on the particle contains a fixed number N_b of neighbor particles. We set $N_b = 40$ in our simulations.

In the following, we show the result of a typical simulation: a cloud of total mass $M = 2.7 \times 10^{13} M_\odot$, and initial values of the β -model $\beta = 0.636$, $r_0 = 134$ kpc, and $\rho_0 = 1.52 \times 10^{-26} \text{ g cm}^{-3}$. The upper left panel of Figure 2 shows that the total energy is conserved to better than 0.1%. The evolution of the gravitational potential, kinetic, thermal and total energies (upper right panel) shows that in half a billion years the system reaches equilibrium and remains confined; in fact, 90% of the mass is within 500 kpc (Figure 3). It follows that in conformal gravity a cloud of gas can easily remain confined without the need of dark matter.

The bottom right panel of Figure 2 shows the evolution of the virial ratio: the sum K of the thermal and kinetic

energy over the total gravitational potential energy W_{tot} . At equilibrium we must have $2K + \sum \mathbf{r}_i \cdot \mathbf{F}_i = 0$, where $\sum \mathbf{r}_i \cdot \mathbf{F}_i = 2W_N - W_{\text{tot}}$ (Section 4). Therefore $K/W_{\text{tot}} = (1/2) - (W_N/W_{\text{tot}})$. From equation 20 we see that W_{tot} is positive and $W_{\text{tot}} \gg |W_N|$ because $(a/R_0)^2 \gg 1$; therefore, unlike Newtonian gravity where $K/W_{\text{tot}} = -1/2$ at equilibrium, here the virial ratio K/W_{tot} is slightly larger than $1/2$.

In the Tree+SPH code each gas particles of mass m_i and density ρ_i carries the electron number density n_{e_i} , and the internal energy u_i . By assuming an optically thin gas of primordial cosmic abundance $X = 0.76$ and $Y = 0.24$, we can estimate the particle temperature T_i ; we also estimate the ion number density $n_{\text{H}_i} + n_{\text{He}_i}$ that we use below. The bottom left panel of Figure 2 shows that the final mass-weighted mean temperature of the system is 90 keV, as expected from the argument provided in Section 4.

Figure 4 shows the density and temperature profiles of the final configuration. As in real clusters, the β -model is still an excellent approximation to the final density profile. The best fit yields $\beta = 1.65$, $r_0 = 142$ kpc and $\rho_0 = 1.6 \times 10^{-25} \text{ g cm}^{-3}$. These parameters roughly agree with typical values of real clusters, although β is $\sim 2 - 3$ times larger than typical values (see, e.g., Markevitch et al. 1999).

The result in strong disagreement with observations is the rising temperature profile shown in the right panel of Figure 4. At large radii, we see that $T \propto r^2$, as anticipated in Section 4.

For completeness, we show the surface brightness and the temperature maps in Figure 5. Each map is an equally spaced $N_p \times N_p$ grid, with $N_p = 128$, corresponding to a length resolution ≈ 15.6 kpc. In the Tree+SPH code, each gas particle has a smoothing length h_i and the thermodynamical quantities it carries are distributed within the sphere of radius h_i according to the compact kernel $W(r; h_i)$, which has the same functional form of the gravitational kernel (see Appendix A), where r is the distance to the particle center. The X-ray surface brightness S_{jk} on the grid point $\{j, k\}$ is

$$S_{jk} = \frac{1}{d_p^2} \sum n_{e_i}(n_{\text{H}_i} + n_{\text{He}_i})\Lambda(T_i)w_i dV_i \quad (26)$$

where d_p^2 is the pixel area, the sum runs over all the particles, and $w_i \propto \int W(x)dl$ is the weight proportional to the fraction of the particle volume $dV_i = m_i/\rho_i$ which contributes to the grid point $\{j, k\}$. For each particle, the weights w_k are normalized to satisfy the relation $\sum w_k = 1$ where the sum is now over the grid points within the particle circle. When h_i is so small that the circle contains no grid point, the particle quantity is fully assigned to the closest grid point. We use the cooling function $\Lambda(T)$ of Sutherland & Dopita (1993). The total X-ray luminosity is

$$L_X = \sum n_{e_i}(n_{\text{H}_i} + n_{\text{He}_i})\Lambda(T_i)dV_i. \quad (27)$$

Given the large equilibrium temperature, the cluster shown in Figure 5 has $L_X = 3.86 \times 10^{46} \text{ erg s}^{-1}$ at equilibrium, an order of magnitude larger than the most luminous X-ray clusters. The temperature whose map is shown in Figure 5 is the emission-weighted temperature

$$T_{jk} = \frac{\sum n_{e_i}(n_{\text{H}_i} + n_{\text{He}_i})\Lambda(T_i)T_i w_i dV_i}{\sum n_{e_i}(n_{\text{H}_i} + n_{\text{He}_i})\Lambda(T_i)w_i dV_i}. \quad (28)$$

This map dramatically shows how the thermal properties of the intracluster medium totally disagree with real clusters.

At this point, we cannot draw our conclusions without the following relevant cautionary tale. The results we show here derive from simulations that treat the gas adiabatically. In other words, we neglect radiative cooling and the gas heating processes due to astrophysical sources, as supernovae explosions, energy injection from active galactic nuclei, or galactic and stellar winds. These heating processes act at different times and with different effectiveness, depending on the detailed history of star and galaxy formation. This history is currently totally unexplored in conformal gravity, and the detailed mechanisms of the heating processes themselves are still poorly understood (e.g., Borgani et al. 2008). Therefore, the appropriate inclusion of these cooling and heating processes in our simulations is beyond the illustrative purpose of this paper.

However, an appropriate interplay between cooling and heating processes could in principle provide a possible route to reconcile conformal gravity with the properties of X-ray clusters. In fact, since our results show that, for the typical gas density of real systems, the gas temperature is an order of magnitude larger than observed, radiative cooling would be very efficient in conformal clusters and the entire intracluster medium could cool in less than 1 Gyr. Effective heating processes would thus be necessary to reheat the intracluster medium to the observed X-ray temperatures. These heating processes must be more efficient in the cluster center than in the cluster outskirts, because the cooling time increases with the clustrocentric radius. However, although we cannot exclude that the various complex physical processes could eventually conspire to reconcile conformal gravity with observations, it is plausible that, in order to provide intracluster media with the observed thermal properties, the cooling and heating processes should be severely fine-tuned during the formation and evolution of clusters and cluster galaxies.

6 CONCLUSION

Conformal gravity can explain the rotation curves of disk galaxies and the current accelerated expansion of the universe without resorting to dark matter and dark energy. We have modified a Tree+SPH code to run hydrodynamical simulations of isolated X-ray galaxy clusters to show that conformal gravity does not share the same success on the scales of clusters.

These simulations confirm our simple analytic estimates that show that gas clouds with mass $\sim 10^{12} - 10^{13} M_{\odot}$, which are typical values of the total mass of the hot gas present in real clusters, remain confined with an equilibrium mean temperature $\sim 10 - 100$ keV, ten times larger than the observed temperatures; more dramatically, because of the presence of a linear term in the gravitational potential, at large clustrocentric radius r , the gas temperature increases with r^2 , rather than decreasing as in real systems.

Our analysis totally neglects radiative cooling and gas heating from astrophysical sources, as supernovae or active galactic nuclei. The interplay between these processes can in principle provide a way to reconcile conformal gravity with observations. It is however unclear if and how much these

processes should be fine-tuned to provide X-ray clusters in agreement with observations.

In addition to this topic, we can see two more open issues whose solution might also reconcile conformal gravity with observations:

(i) In conformal gravity, all the matter in the universe is expected to affect the local dynamics. The net effect is to contribute a constant inward acceleration $-GM_0/R_0$ in addition to the gravitational acceleration generated by local sources. Because we included this constant acceleration in our simulations, we could neglect the rest of the universe and impose vacuum boundary conditions. It might be possible that assimilating the gravitational influence of the nearby matter surrounding the X-ray cluster in the constant “universe” acceleration $-GM_0/R_0$ is inappropriate: in fact, nearby external matter might decrease the gravitational attraction of the interior matter and hopefully reduce the thermal energy of the gas. To appropriately investigate this effect, we should simulate the dynamics of large-scale structure within a full cosmological context. However, this task is not trivial just because the gravitational field is highly non-local. This investigation would also benefit from the implementation into the numerical simulation of the yet unavailable theory of structure formation.

(ii) The gravitational potential we implemented in our simulations derives from a metric where the conformal invariance is broken by an arbitrary choice of the conformal factor $\Omega^2(x)$. It is unclear whether this choice provides a coordinate system whose physics describes the real world or it is an artifact of the reference frame. It also remains to be seen whether a spontaneous breaking of the conformal invariance, in theories where matter and gravity are conformally coupled (Edery et al. 2006), can provide a metric, and thus a gravitational potential, where the observed thermal properties of the intracluster medium can be reproduced.

In Section 1 we mentioned that the nucleosynthesis of light elements and the phenomenology of gravitational lensing are two open issues that need to be solved before accepting conformal gravity as a viable alternative theory of gravity and cosmology. Here, we have shown that the thermodynamics of X-ray clusters poses a third challenge to this theory.

ACKNOWLEDGMENTS

We thank Volker Springel for making public his superb Tree+SPH code and the referee whose careful report prompted us to clarify some aspects of our results. We acknowledge vivid discussions with Jörg Colberg, Keith Horne and Philip Mannheim on very early versions of this work. Support from the PRIN2006 grant “Costituenti fondamentali dell’Universo” of the Italian Ministry of University and Scientific Research and from the INFN grant PD51 is gratefully acknowledged.

REFERENCES

- Barabash O. V., Pyatkovska H. P. 2007, arXiv:0709.1044v1
 Barabash O. V., Shtanov Yu. V. 1999, PRD, 60, 064008
 Bekenstein J. D. 2006, Contemp. Phys., 47, 387
 Bender C. M., Mannheim P. D. 2008, PRL, 100, 110402
 Böhmer C. G., Harko T., Lobo F. S. N. 2008, JCAP, 03, 024
 Borgani S., Diaferio A., Dolag K., Schindler S. 2008, Sp. Sci. Rev., 134, 269
 Capozziello S., Francaviglia M. 2008, Gen. Relativ. and Grav., 40, 357
 Copeland E. J., Sami M., Tsujikawa S. 2006, Int. J. Mod. Phys. D, 15, 1753
 Edery A. 1999, PRL, 83, 3990
 Edery A., Fabbri L., Paranjape M.B. 2006, Class. Quant. Grav., 23, 6409
 Edery A., Méthot A.A., Paranjape M.B. 2001, Gen. Relativ. and Grav., 33, 2075
 Edery A., Paranjape M.B. 1998, PRD, 58, 4011
 Edery A., Paranjape M.B. 1999, Gen. Relativ. and Grav., 31, 1031
 Elizondo D., Yepes G. 1994, ApJ, 428, 17
 Flanagan E. E. 2006, PRD, 74, 023002
 Fujii Y., Maeda K. 2003, The scalar-tensor theory of gravitation, Cambridge University Press
 Horne K. 2006, MNRAS, 369, 1667
 Inoue S., Iwamoto N., Orito M., Terasawa M. 2003, ApJ, 595, 294
 Knox L., Kosowsky A. 1993, arXiv:astro-ph/9311006
 Maartens R. 2004, Living Rev. Rel., 7, 7
 Mannheim P. D. 1990, Gen. Relativ. and Grav., 22, 289
 Mannheim P. D. 1993, ApJ, 419, 150
 Mannheim P. D. 1997, ApJ, 479, 659
 Mannheim P. D. 2001, ApJ, 561, 1
 Mannheim P. D. 2003, Int. J. Mod. Phys. D, 12, 893
 Mannheim P. D. 2006, Prog. in Part. and Nucl. Phys., 56, 340
 Mannheim P. D. 2007, PRD, 75, 124006
 Mannheim P. D. 2008a, arXiv:0707.2283
 Mannheim P. D. 2008b, arXiv:0809.1200
 Mannheim P. D. Kazanas D., 1989, ApJ, 342, 635
 Mannheim P. D. Kazanas D., 1994, Gen. Relativ. and Grav., 26, 337
 Markevitch M., Vikhlinin A., Forman W. R., Sarazin C. L. 1999, ApJ, 527, 545
 Mullan D. J., Linsky J. L. 1999, ApJ, 511, 502
 Navia C. E., Augusto C. R. A., Tsui K. H. 2008, arXiv:0807.0590
 Nojiri S., Odintsov S. D. 2008, arXiv:0807.0685
 Pireaux S. 2004a, Class. Quant. Grav., 21, 1897
 Pireaux S. 2004b, Class. Quant. Grav., 21, 4317
 Prodanovic T., Fields B. D. 2003, ApJ, 597, 48
 Rood H. J., Sastry G. N. 1971, PASP, 83, 313
 Springel V. 2005, MNRAS, 364, 1105
 Springel V., Yoshida N., White S. D. M. 2001, New Astronomy, 6, 51
 Sutherland R. S., Dopita M. A. 1993, ApJS, 88, 253
 Varieschi G. U. 2008, arXiv:0809.4729
 Walker M.A. 1994, ApJ, 430, 463
 Wei H., Zhang S. N. 2008, arXiv:0808.2240
 Weyl H. 1918, Math. Z., 2, 384
 Weyl H. 1919, Ann. Phys. Lpz., 59, 101
 Weyl H. 1920, Phys. Z., 21, 649
 White S. D. M., Navarro J. F., Evrard A. E., Frenk C. S. 1993, Nature, 366, 429

APPENDIX A: THE SOFTENING KERNEL

The publicly available code GADGET-1.1 (Springel et al. 2001; Springel 2005) is a Tree+SPH code which integrates the equations of motion of N particles which interact gravitationally. The particles are a discrete representation of either a collisionless or a collisional fluid. Here, we consider only adiabatic processes and neglect the possibility of radiative cooling of the collisional fluid.

The only modification to the code we need is the computation of the gravitational potential ϕ and its corresponding acceleration. At position \mathbf{r} , N particles of mass m_i at position \mathbf{x}_i generates the potential

$$\phi(\mathbf{r}) = G \sum_{i=1}^N \left[-m_i g_N(y_i) + \frac{m_i}{R_0^2} g_{CM}(y_i) + \frac{M_0}{R_0^2} g_{CC}(y_i) \right] \quad (\text{A1})$$

where $y_i = |\mathbf{r} - \mathbf{x}_i|$. For point sources, $g_N(y) = 1/y$ and $g_{CM}(y) = g_{CC}(y) = y$. The acceleration $\mathbf{a}(\mathbf{r}) = -\nabla\phi(\mathbf{r})$ is

$$\mathbf{a}(\mathbf{r}) = G \sum_{i=1}^N \mathbf{y}_i \left[m_i g_N^1(y_i) - \frac{m_i}{R_0^2} g_{CM}^1(y_i) - \frac{M_0}{R_0^2} g_{CC}^1(y_i) \right] \quad (\text{A2})$$

where $g_N^1(y)y = dg_N/dy$, and analogously for g_{CM}^1 and g_{CC}^1 .

GADGET-1.1 treats particles as extended spherical objects with mass m and density profile $\rho(r) = mW(r;h)$ where

$$W(r;h) = \frac{8}{\pi h^3} \begin{cases} 1 - 6x^2 + 6x^3 & 0 \leq x < \frac{1}{2} \\ 2(1-x)^3 & \frac{1}{2} \leq x < 1 \\ 0 & x \geq 1, \end{cases}$$

where $x = r/h$. $W(r;h)$ is a spline kernel which avoids unrealistic divergences of the Newtonian acceleration for arbitrary small particle separations.

The spline kernel implies that each particle is not a point source of gravitational potential. Rather, its gravitational potential is correctly computed as an extended source of density $W(r;h)$. According to equation (15) we find, with $u = y/h$,

$$g_N(y;h) = \frac{1}{h} \begin{cases} \frac{14}{5} - \frac{16}{3}u^2 + \frac{48}{5}u^4 - \frac{32}{5}u^5 & 0 \leq u < \frac{1}{2} \\ -\frac{1}{15u} + \frac{16}{3} - \frac{32}{3}u^2 + 16u^3 & \frac{1}{2} \leq u < 1 \\ \frac{1}{u} & u \geq 1, \end{cases}$$

$$g_N^1(y;h) = \frac{1}{h^3} \begin{cases} -\frac{32}{3} + \frac{192}{5}u^2 - 32u^3 & 0 \leq u < \frac{1}{2} \\ \frac{1}{15u^3} - \frac{64}{3} + 48u - \frac{192}{5}u^2 & \frac{1}{2} \leq u < 1 \\ -\frac{1}{u^3} & u \geq 1, \end{cases}$$

$$g_{CM}(y;h) = h \begin{cases} \frac{31}{70} + \frac{14}{15}u^2 - \frac{8}{15}u^4 + \frac{16}{35}u^6 & 0 \leq u < \frac{1}{2} \\ -\frac{1}{840u} + \frac{16}{35} - \frac{u}{15} + \frac{16}{15}u^2 & \frac{1}{2} \leq u < 1 \\ u + \frac{3}{40u} & u \geq 1, \end{cases}$$

$$g_{CM}^1(y;h) = \frac{1}{h} \begin{cases} \frac{28}{15} - \frac{32}{15}u^2 + \frac{96}{35}u^4 - \frac{8}{5}u^5 & 0 \leq u < \frac{1}{2} \\ \frac{1}{840u^3} - \frac{1}{15u} + \frac{32}{15} - \frac{64}{15}u^2 & \frac{1}{2} \leq u < 1 \\ \frac{1}{u} - \frac{3}{40u^3} & u \geq 1, \end{cases}$$

$g_{CC} = y$, and $g_{CC}^1 = 1/y$.